ACADEMIC PRESS

Available online at www.sciencedirect.com

SCIENCE DIRECT®

Journal of Sound and Vibration 261 (2003) 715–727

JOURNAL OF SOUND AND VIBRATION

www.elsevier.com/locate/jsvi

Crack detection in beams by wavelet analysis of transient flexural waves

Jiayong Tian, Zheng Li, Xianyue Su*

Department of Mechanics and Engineering Science, Peking University, Beijing, 100871, People's Republic of China

Received 16 January 2001; accepted 30 May 2002

Abstract

In this paper, a method of crack detection in beam is provided by wavelet analysis of transient flexural wave. Firstly, we introduce a rotational spring in the cracked-beam model, and calculate the transient flexural wave propagation by the Reverberation Matrix Method. Secondly, at any point in this beam, the arrival time of waves with different group velocities can be identified by means of analysis of wavelet transform. From the signal of mid-frequency flexural wave extracted by wavelet transform, we can exactly determine the existence and position of crack in the beam. Here, a similar experiment is also produced to test the transient strain signal in beam, and the result after wavelet transform analysis is shown in accord with the theoretical one. Therefore, a powerful method is proved by the theoretical and experimental studies on the cracked beam, which can detect the crack accurately utilizing the wavelet analysis of the mid-frequency flexural wave.

1. Introduction

Defects are almost unavoidable in structures, and their existences will decrease the mass, stiffness, strength and safety of structures. How to diagnose the existence and position of defect is an important and promising problem. Currently, a lot of researchers devote their attention to detect the damage in structure by means of the ultrasonic method [1] and vibration-based method [2–5]. Because the ultrasonic wave decays very quickly during the propagating process in structure, it can only detect the damage in its near field for the case that the vicinity of damage must be known in advance. For the damage detection in a large-scale structure, the ultrasonic method will be time-consuming and costly. The vibration-based method utilizes the vibration

*Corresponding author. Fax: +86-10-62759378.
E-mail address: xysu@mech.pku.edu.cn (X. Su).

0022-460X/03/$ - see front matter
PII: S0022-460X(02)01001-5

characteristic of structure to diagnose the damage, which can only give global information on the structure. Rizos and Apragathos [3] produced the crack in beam as a local flexibility and developed a crack detective method by the measured vibration modes to determine the crack location and depth. Narkis [4] stimulated the crack in simply supported beam by an equivalent spring and investigated the change of natural frequency to identify the crack location. However, the signal of vibration is insensitive to damage, especially to small damage. Therefore, a new detective method needs to be proposed, which not only is sensitive to small damage, but also can detect the damage in large-scale structures. Consider the middle frequency wave which not only is sensitive to the damage but also decays slowly unlike the ultrasonic wave utilizing the middle frequency signal to diagnose the damage will be an effective method, and up to now only a little attempt has been done [6].

Wavelet transform (WT) is the local transform of space and time. Time–frequency window of WT has self-adaptability, which is suitable for detecting the abrupt information from signal. Inoue et al. [7] firstly applied the Morlet wavelet transform to the analysis of flexural wave in Euler beam. Onsay and Haddow [8] determined the location of the impact by analyzing the flexural wave of Timosenko beam based on Gabor wavelet. They point out that the largest peak of WT magnitude of dispersive wave happens at the arrival time of wave at the group velocity. However, the above works are not related to the damage detection.

The aim of this paper is to give a global damage detective method based on wavelet analysis of flexural wave in beams. Firstly, we introduce an approximate model of Timoshenko beam including a vertical edge crack, where the crack is modelled by a rotational spring. According to this model, transient flexural waves can be calculated by the Reverberation Matrix Method [9,10]. Furthermore, based on the wavelet analysis of the flexural wave in cracked beam and non-cracked beam, we can identify the arrival time of waves with different group velocities, and determine the location of crack in the beam. Lastly, a similar experiment is given to verify the reliability of this method.

2. Cracked beam model

For convenience, we consider a Timoshenko rectangular beam with a single-edge vertical crack as shown in Fig. 1. Here the cracked beam is treated as two uniform beams, and connected by a rotational spring at the crack location. In order to avoid the non-linearity, the crack is assumed to be open at any time, and only the effect around near field of crack is considered. We decompose

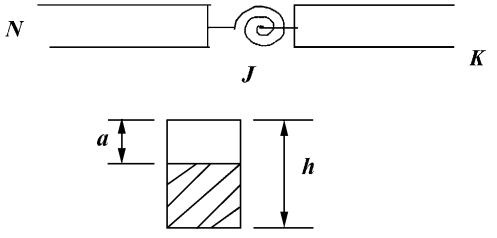

Fig. 1. The model of crack.

the transverse displacement w into w_b caused by bending and w_s caused by shear force, so the flexural wave equations of Timoshenko beam can be written as follows:

$$\kappa GA\frac{\partial^2 w_s}{\partial x^2} = \rho A\frac{\partial^2 (w_b + w_s)}{\partial t^2},$$
$$EI_z\frac{\partial^3 w_b}{\partial x^3} + AG\frac{\partial w_s}{\partial x} = \rho I_z\frac{\partial^3 w_b}{\partial t^2 \partial x}, \tag{1}$$

where E is Young's modulus, G the shear modulus, ρ the material density, and κ the shear force factor. I_z and A indicate the moment of inertial and the area of cross-section, respectively. The corresponding moment, shear force, displacement and rotational angle is given by

$$M = EI_z\frac{\partial^2 w_b}{\partial x^2}, \qquad V = \kappa GA\frac{\partial w_s}{\partial x}, \qquad w = w_b + w_s, \qquad \psi = \frac{\partial w_b}{\partial x}. \tag{2}$$

The group velocity of wave can be defined by

$$c_g = \mathrm{d}\omega/\mathrm{d}k, \tag{3}$$

where ω is the angular frequency and k is the wave number.

There are two kinds of waves with different group velocities in Timoshenko beam as shown in Fig. 2. One kind of waves (slow wave) has a lower limit of group velocity and can propagate at all frequencies. The other one (fast wave) has a higher limit of group velocity, but it can only propagate beyond the cut-off frequency, which is expressed by

$$\omega_c = c_1/R_z\sqrt{\eta}, \tag{4}$$

where $\eta = E/\kappa G$, $c_1 = \sqrt{E/\rho}$, $R_z = \sqrt{I_z/A}$.

The connective conditions of two uniform beams at the crack are

$$w_{JK} = w_{JN}, \quad M_{JK} = M_{JN}, \quad V_{JK} = V_{JN}, \quad \psi_{JK} - \psi_{JN} = Cw''_{bJK}, \tag{5}$$

where C is the flexibility of the rotational spring. Subscripts JK and JN indicate the point J on the crack corresponding to different parts of beam K and N (shown in Fig. 1). The flexibility C for one side crack is given as [3]

$$C = 5.346hf(\xi), \tag{6}$$

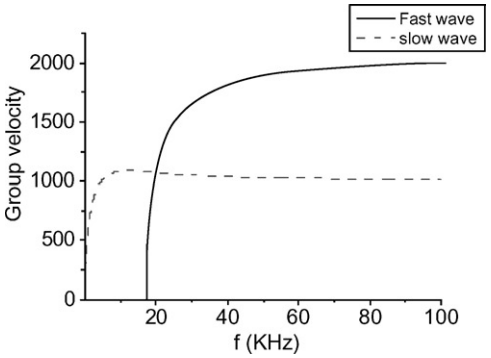

Fig. 2. Group velocity in Timoshenko beam.

where $\xi = a/h$, h is the height of the cross-section of the beam, a is the depth of the crack,

$$f(\xi) = 1.8624\xi^2 - 3.95\xi^3 + 16.375\xi^4 - 37.226\xi^5 + 76.81\xi^6 - 126.9\xi^7 + 172\xi^8 - 143.97\xi^9 + 66.56\xi^{10}$$

3. Transient flexural wave of cracked beam

Consider that a cracked beam can be separated into M elements by $M+1$ joints. All external forces are assumed to be loaded at joints. The crack is also considered as a joint. For an element JN, we introduce a local co-ordinate system at each joint, which is shown in Fig. 3.

By applying Laplace transform to Eqs. (1) and (2), where Laplace transform of (w^{JN}, ψ^{JN}) with respect to t is denoted by $(\hat{w}^{JN}, \hat{\psi}^{JN}) = \int_0^{+\infty} (w^{JN}, \psi^{JN})\, e^{-pt}\, dt$, the corresponding displacement vector $\hat{\boldsymbol{U}}^{JN}(x,p) = \{\hat{w}^{JN}(x,p), \hat{\psi}^{JN}(x,p)\}^T$ in the local co-ordinate system JN is expressed as

$$\hat{\boldsymbol{U}}^{JN}(x,p) = \boldsymbol{A}_u^{JN}\hat{\boldsymbol{a}}^{JN} + \boldsymbol{D}_u^{JN}\hat{\boldsymbol{d}}^{JN}, \tag{7}$$

where $\hat{\boldsymbol{a}}^{JN} = \{\hat{a}_1^{JN}, \hat{a}_2^{JN}\}^{JN}$ and $\hat{\boldsymbol{d}}^{JN} = \{\hat{d}_1^{JN}, \hat{d}_2^{JN}\}^{JN}$ are amplitude of arriving and departing waves in the local co-ordinate system JN, respectively. The phase matrix of the arriving and the departing displacement wave $\boldsymbol{A}_u^{JN}$ and $\boldsymbol{D}_u^{JN}$ in the local co-ordinate system JN are denoted by

$$\boldsymbol{A}_u^{JN} = \begin{bmatrix} (1+\alpha_1)e^{s_1 x} & (1+\alpha_2)e^{s_2 x} \\ s_1 e^{s_1 x} & s_2 e^{s_2 x} \end{bmatrix}, \qquad \boldsymbol{D}_u^{JN} = \begin{bmatrix} (1+\alpha_1)e^{-s_1 x} & (1+\alpha_2)e^{-s_2 x} \\ -s_1 e^{-s_1 x} & -s_2 e^{-s_2 x} \end{bmatrix}, \tag{8}$$

where

$$s_{1,2} = p\sqrt{1+\eta \pm \sqrt{(1-\eta)^2 - 4(\eta + c_1^2/(R_z p)^2}}/\sqrt{2}c_1,\ \alpha_{1,2} = R_Z^2(p^2 - c_1^2 s_{1,2}^2)/(\kappa c_2^2),\ c_2 = \sqrt{G/\rho}.$$

Force vector $\hat{\boldsymbol{F}}^{JN}(x,p) = \{\hat{M}_z^{JN}(x,p), \hat{V}_z^{JN}(x,p)\}^T$ in the local co-ordinate JN is expressed as

$$\hat{\boldsymbol{F}}^{JN}(x,p) = \boldsymbol{A}_f^{JN}\hat{\boldsymbol{a}}^{JN} + \boldsymbol{D}_f^{JN}\hat{\boldsymbol{d}}^{JN}, \tag{9}$$

where $\boldsymbol{A}_f^{JN}$ and $\boldsymbol{D}_f^{JN}$ are the phase matrix of the arriving and the departing force wave, which are

$$\boldsymbol{A}_f^{JN} = \begin{bmatrix} EI_z s_1^2 e^{s_1 x} & EI_z s_2^2 e^{s_2 x} \\ kAG\alpha_1 s_1 e^{s_1 x} & kAG\alpha_2 s_2 e^{s_2 x} \end{bmatrix}, \qquad \boldsymbol{D}_f^{JN} = \begin{bmatrix} EI_z s_1^2 e^{-s_1 x} & EI_z s_2^2 e^{-s_2 x} \\ -kAG\alpha_1 s_1 e^{-s_3 x} & -kAG\alpha_2 s_2 e^{-s_2 x} \end{bmatrix}. \tag{10}$$

Substituting Eqs. (7) and (9) into the boundary condition Eq. (5) at the crack, force equilibrium and displacement compliance for other joints, and introducing the arriving wave amplitude vector

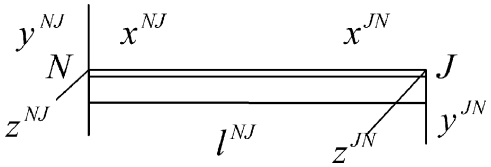

Fig. 3. The local co-ordinate system of joint.

$\hat{\boldsymbol{a}}^J = \{\hat{\boldsymbol{a}}^{JN}, \hat{\boldsymbol{a}}^{JK}\}^{\mathrm{T}}$ and departing wave amplitude vector $\hat{\boldsymbol{d}}^J = \{\hat{\boldsymbol{d}}^{JN}, \hat{\boldsymbol{d}}^{JK}\}^{\mathrm{T}}$ of Joint J, the scattering relation of the arriving and the departing wave of Joint J has the form

$$\hat{\boldsymbol{d}}^J = \boldsymbol{S}^J \hat{\boldsymbol{a}}^J - \hat{\boldsymbol{s}}^J, \tag{11}$$

where $\boldsymbol{S}^J$ is the local scatter matrix of Joint J. $\hat{\boldsymbol{s}}^J$ is the local source vector of Joint J, which can be found in the Appendix.

Then the scatter relation of all joints is assembled into the global matrix as

$$\hat{\boldsymbol{d}} = \boldsymbol{S}\hat{\boldsymbol{a}} + \hat{\boldsymbol{s}}, \tag{12}$$

where $\hat{\boldsymbol{d}}$, $\hat{\boldsymbol{a}}$, $\hat{\boldsymbol{s}}$ and $\boldsymbol{S}$ are, respectively, the global amplitude vectors of arriving wave and departing wave, source vector and scatter matrix. Since both vectors $\hat{\boldsymbol{d}}$ and $\hat{\boldsymbol{a}}$ are unknown quantities, there must be an additional equation relating $\hat{\boldsymbol{d}}$ and $\hat{\boldsymbol{a}}$. A departing wave from a joint of a beam is also considered as an arriving wave at the other joint of the same beam. However, the amplitude for waves at both joints of element JN can be differed by a phase shift factor as follows:

$$\hat{\boldsymbol{a}}^{JN} = \boldsymbol{P}^{JN}(l^{JK}, p)\hat{\boldsymbol{d}}^{NJ}, \tag{13}$$

where $\boldsymbol{P}^{JN}(l^{JN}, p)$ is the local phase shift matrix in the local co-ordinate system JN, which is

$$\boldsymbol{P}^{JN}(l^{JN}, p) = \begin{bmatrix} -\mathrm{e}^{-s_1 l^{JN}} & 0 \\ 0 & -\mathrm{e}^{-s_2 l^{JN}} \end{bmatrix}. \tag{14}$$

Then Eq. (14) can be assembled into the global matrix as

$$\hat{\boldsymbol{a}} = \boldsymbol{P}\tilde{\boldsymbol{d}}, \tag{15}$$

where $\boldsymbol{P}$ is the global phase shift matrix, which is given by

$$\boldsymbol{P} = \begin{bmatrix} \boldsymbol{P}^{12}(l^{12}, p) & 0 & \cdots & 0 & 0 \\ 0 & \boldsymbol{P}^{21}(l^{21}, p) & \cdots & 0 & 0 \\ \vdots & \vdots & \ddots & \vdots & \vdots \\ 0 & 0 & \cdots & \boldsymbol{P}^{M(M+1)}(l^{M(M+1)}, p) & 0 \\ 0 & 0 & \cdots & 0 & \boldsymbol{P}^{(M+1)M}(l^{(M+1)M}, p) \end{bmatrix}. \tag{16}$$

The global vectors $\tilde{\boldsymbol{d}}$ and $\hat{\boldsymbol{d}}$ have the same elements, but are sequenced in different vectors. This relation can be expressed through a permutation matrix $\boldsymbol{H}$ as

$$\tilde{\boldsymbol{d}} = \boldsymbol{H}\hat{\boldsymbol{d}}, \tag{17}$$

where $\boldsymbol{H}$ is a $4M \times 4M$ block-diagonal matrix composed of M, the same 4×4 sub-matrix $\boldsymbol{H}_1$ and other vanishing elements as follows:

$$\boldsymbol{H} = \begin{bmatrix} \boldsymbol{H}_1 & 0 & \cdots & 0 \\ 0 & \boldsymbol{H}_1 & \cdots & 0 \\ \vdots & \vdots & \ddots & \vdots \\ 0 & 0 & \cdots & \boldsymbol{H}_1 \end{bmatrix}, \qquad \boldsymbol{H}_1 = \begin{bmatrix} 0 & 0 & 1 & 0 \\ 0 & 0 & 0 & 1 \\ 1 & 0 & 0 & 0 \\ 0 & 1 & 0 & 0 \end{bmatrix}. \tag{18}$$

Substituting Eq. (17) into Eq. (15), the additional equation about $\hat{\boldsymbol{d}}$ and $\hat{\boldsymbol{a}}$ is derived as

$$\hat{\boldsymbol{a}} = \boldsymbol{PH}\hat{\boldsymbol{d}}. \tag{19}$$

Solving Eqs. (19) and (12), the result can be written as

$$\hat{\boldsymbol{d}} = [\boldsymbol{I} - \boldsymbol{R}]^{-1}\hat{\boldsymbol{s}}, \tag{20}$$

where $\boldsymbol{R} = \boldsymbol{SPH}$ is called the Reverberation Matrix.

If $\hat{\boldsymbol{d}}$ and $\hat{\boldsymbol{a}}$ are known, the displacement and the force in Laplace domain at any position yield

$$\begin{aligned}\hat{\boldsymbol{U}} &= (\boldsymbol{A}_u\boldsymbol{PH} + \boldsymbol{D}_u)[\boldsymbol{I} - \boldsymbol{R}]^{-1}\hat{\boldsymbol{s}},\\ \hat{\boldsymbol{F}} &= (\boldsymbol{A}_f\boldsymbol{PH} + \boldsymbol{D}_f)[\boldsymbol{I} - \boldsymbol{R}]^{-1}\hat{\boldsymbol{s}}.\end{aligned} \tag{21}$$

It can be solved by inverse Laplace transform of Eq. (21), but it is not easy to solve. Because $[\boldsymbol{I} - \boldsymbol{R}]^{-1}$ has a lot of poles solved by residual theorem, it needs a lot of accurate poles, which makes the computational work become very difficult. If the matrix $I - R$ is a singular one, $[\boldsymbol{I} - \boldsymbol{R}]^{-1}$ does not exist. By the expansion of rays, it can be the expanded series $[\boldsymbol{I} - \boldsymbol{R}]^{-1} = \sum_{K=0}^{\infty}\boldsymbol{R}^K$, so the displacement vector is denoted as

$$\boldsymbol{U}(x,t) = \sum_{K=0}^{\infty}\frac{1}{2\pi\mathrm{j}}\int[\boldsymbol{A}_u\boldsymbol{PH} + \boldsymbol{D}_u]\boldsymbol{R}^K\hat{s}\mathrm{e}^{pt}\,\mathrm{d}p, \tag{22}$$

Here, each integral represents the waves which arrive at point x after being refracted K times in the beam. The waves with respect to $K = 0$ arrive directly at x point from source, so they are called source waves. According to the observation time, the dynamic response can be computed by truncating the series. The inverse Laplace transform of Eq. (22) can be computed by means of the Fast Fouier Transform (FFT) according to Ref. [10].

4. Wavelet analysis

Let $f(t)$ be a signal in the time domain $(-\infty, \infty)$, continuous wavelet transform of $f(t)$ can be expressed as

$$Wf(a,b) = \frac{1}{\sqrt{a}}\int_{-\infty}^{\infty} f(t)\bar{\phi}\left(\frac{t-b}{a}\right)\mathrm{d}t, \tag{23}$$

where φ is mother wavelet and the bar indicates its complex conjugate. a and b are real-valued parameters and can be used to characterize the dilation and translation features of wavelet.

In this paper, Morlet wavelet and its Fourier transform are adopted, which are

$$\phi(t) = \pi^{-1/4}(\mathrm{e}^{-\mathrm{i}\omega_0 t} - \mathrm{e}^{-\omega_0^2/2})\mathrm{e}^{-t^2/2}, \qquad \hat{\phi}(\omega) = \pi^{-1/4}(\mathrm{e}^{-(\omega-\omega_0)^2/2} - \mathrm{e}^{-(\omega_0^2+\omega^2)/2}), \tag{24}$$

where ω_0 is a real and positive constant. When $\omega_0 \geqslant 5$, $\mathrm{e}^{-\omega_0^2/2}$ is approximately equal to zero. So Eq. (24) are approximately expressed as

$$\phi(t) = \pi^{-1/4}\mathrm{e}^{-\mathrm{i}\omega_0 t}\mathrm{e}^{-t^2/2}, \qquad \hat{\phi}(\omega) = \pi^{-1/4}\mathrm{e}^{-(\omega-\omega_0)^2/2}. \tag{25}$$

In this paper, we take $\omega_0 = 5$ for the following analysis.

The wave in beams is denoted in the Fourier integral form

$$u(x,t)=\frac{1}{2\pi}\int_{-\infty}^{\infty}A(\omega)\mathrm{e}^{-\mathrm{i}kx+\mathrm{i}\omega t}\,\mathrm{d}t. \tag{26}$$

So WT of $u(x,t)$ can be expressed as

$$Wu(a,b,x)=\frac{\sqrt{a}}{2\pi}\pi^{-1/4}\int_{-\infty}^{\infty}A(\omega)\mathrm{e}^{-\mathrm{i}kx+\mathrm{i}\omega b}\mathrm{e}^{-(a\omega-\omega_0)^2/2}\,\mathrm{d}\omega. \tag{27}$$

For the above equation, only the vicinity of ω_0/a can contribute to the integral of the equation. So Eq. (27) can be expressed approximately as

$$|Wu(a,b,x)|\approx\frac{\pi^{-1/4}}{2\pi\sqrt{a}}A(\omega_0/a)\left|\frac{\sin(Y)}{Y}\right|, \tag{28}$$

where $Y=(k_0'x-b)/a$, $k_0'=\mathrm{d}k/\mathrm{d}\omega|_{\omega=\omega_0/a}$. Eq. (28) indicates that the magnitude of WT takes its maximum value at $a=\omega_0/\omega$ and $b=(\mathrm{d}k/\mathrm{d}\omega)x=x/c_g$. That is to say, the location of peak indicates the arrival time $b=x/c_g$ of the wave with angular frequency $\omega=\omega_0/a$.

5. Numerical example

A cantilever beam with a length of 0.6 m and a cross-section of $0.01\,\mathrm{m}\times0.01\,\mathrm{mm}^2$ is only taken for example in this paper. The material parameters are chosen as modulus of elasticity $E=2.1\times10^{11}$ Pa, the Poisson ratio $v=0.3$ and shear force factor $\kappa=\pi^2/12$. The edge crack with the depth of 0.005 m is located in the middle of the beam. When the step load $F_0H(t)$ is acted on the free end of the beam, strain signals at position A and B in beam can be computed, here A and B points are separately set with the distances from the free end 0.45 and 0.15 m. The transient strain wave of the cracked beam and uncracked beam at A and B is shown in Figs. 4 and 5, respectively, which is computed by the Reverberation Matrix Method. In Figs. 4 and 5, the strain signal and time are normalized by F_0/EA and $L/6c_1$, respectively, where L is the length of the beam. Here, there are 2048 data points recorded as strain signal in the 15 time units.

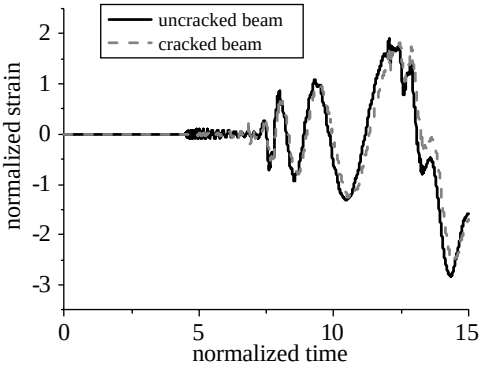

Fig. 4. Strains of position A in uncracked beam and cracked beam.

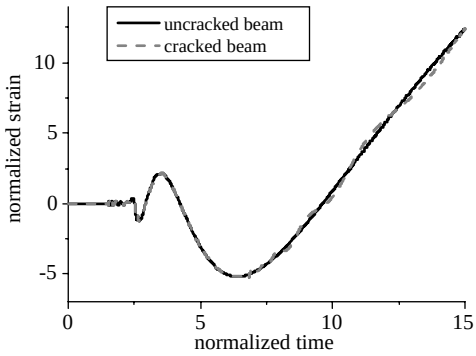

Fig. 5. Strains of position B in uncracked beam and cracked beam.

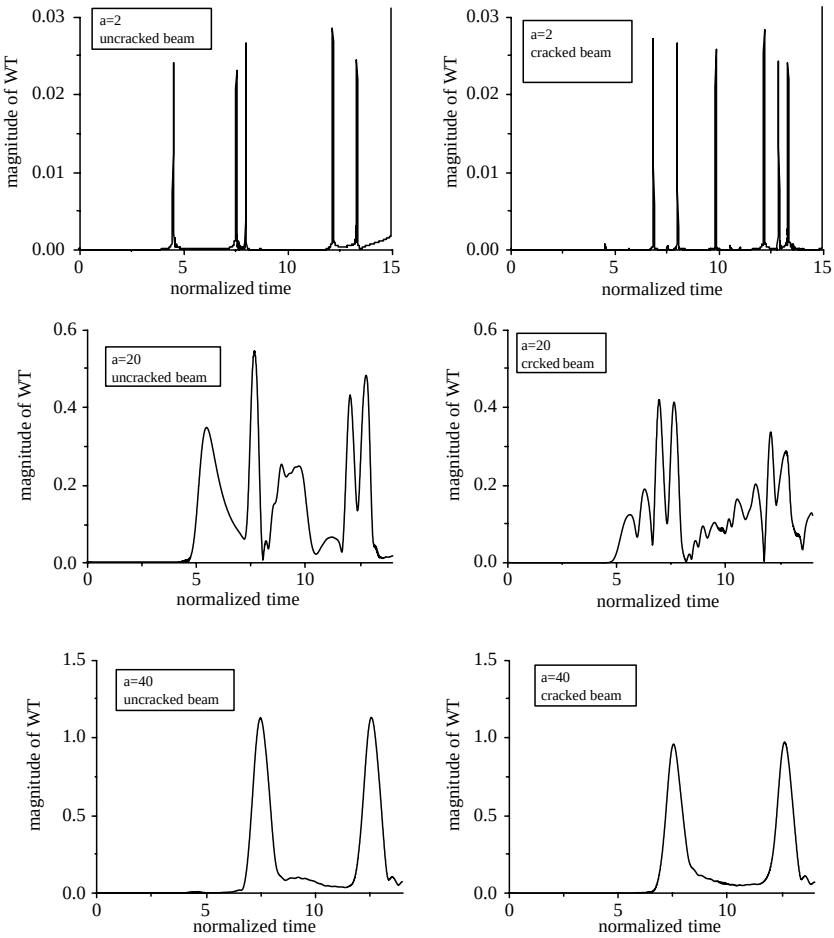

Fig. 6. Magnitude of WT of waves (shown in Fig. 4) with the different normalized scale.

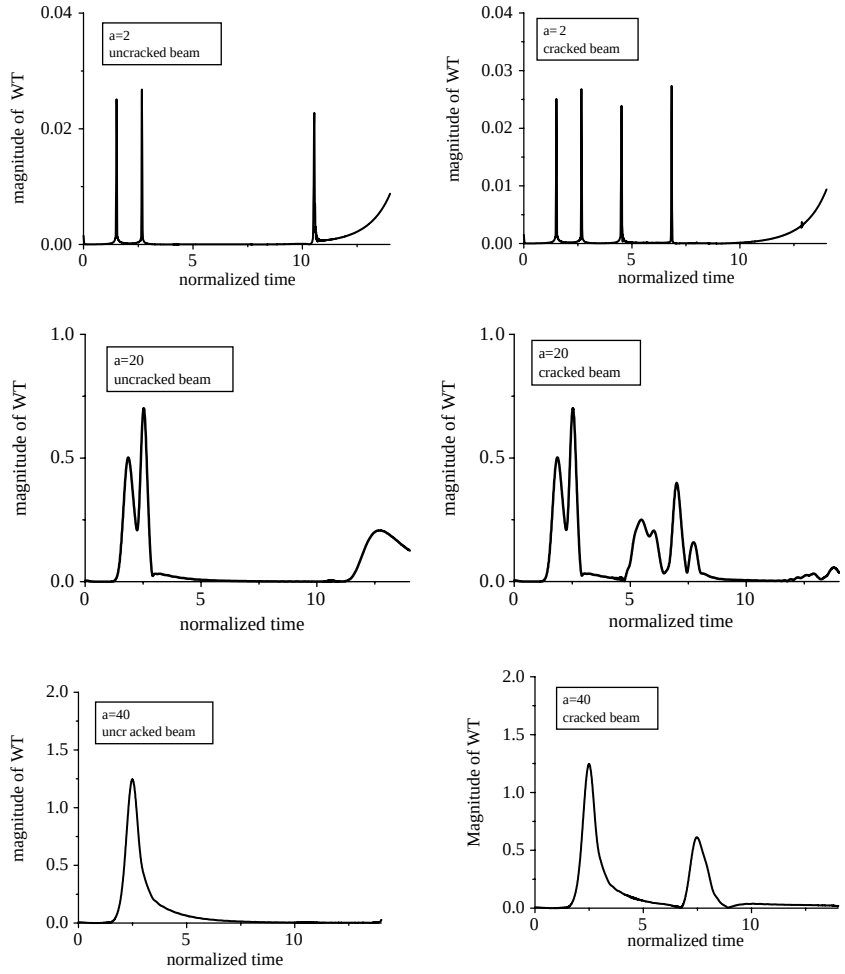

Fig. 7. Magnitude of WT of waves (shown in Fig. 5) with the different normalized scale.

The scale a is also normalized by sampling period T. According to the waves shown in Figs. 4 and 5, their wavelet transform with different normalized scale a is given in Figs. 6 and 7, respectively. Every peak in the figures represents the arrival time of wave at the group velocity. In Fig. 6, for uncracked beam at normalized scale $a = 2$, the times of the first three peaks are separately 4.5264, 7.5366, 8.0054 to time unit, which indicate the arrival of the fast wave directly from the free end, the refracted fast wave from the fixed end, and the slow wave directly from the free end, respectively. The group velocity of the fast wave is 0.9924 and the group velocity of the slow wave is 0.5621. Compared with the uncracked beam, we can notice that WT of cracked beam adds two additional peaks between the first and the second peak to uncracked beam, whose corresponding times are 5.6860, 6.8457. The first additional peak represents the arrival of the refracted slow wave caused by the source fast wave propagating through the crack. But it is too weak as shown in the figure. The second additional peak is the arrival of the refracted fast wave

that is caused by the source slow wave propagating through the crack. To point B, similar results of WT analysis can be obtained as shown in Fig. 7.

Accompanied by the increase of scale a, i.e., the decrease of frequency, width of every peak becomes more and more wide so that some waves are difficult to be identified according to the peak. When the scale is near the normalized cut-off scale (here normalized cut-off scale $a_c = 35$), the group velocity of the fast wave is very low or vanish so that it is not clear to find the peaks representing the arrival of the fast wave and only the slow wave is left. In Figs. 6 and 7, we only can find the peaks representing the slow wave for normalized scale $a = 40$. Compared with the sub-figures of Fig. 7 with normalized scale $a = 40$ for uncracked-beam, the sub-figure of cracked-beam has an additional peak. This peak represents the arrival of slow wave reflected by crack. When the frequency continues to decrease, that is to say, the normalized scale continues to increase; it is more and more difficult to find peaks indicating waves caused by the crack because of the effect of diffraction.

6. Crack localization

Through the above analysis, the method of determining the existence and location of crack based on the wavelet analysis of mid-frequency flexural wave is developed. This process can be shown as follows.

Step 1: Select the appropriate normalized scale a. Here we select the normalized scale greater than or equal to the normalized cut-off scale, which is expressed as

$$a = \omega_0/(\omega_c T), \tag{29}$$

where T is the sampling period.

Step 2: Determine the group velocity of mid-frequency slow wave. According to the first arrival time of the wave at different positions A and B at the selected normalized scale, the group velocity can be calculated by

$$c_g = (l_A - l_B)/(t_A - t_B). \tag{30}$$

Step 3: Give the arrival time of all waves of the uncracked beam according to group velocity of slow wave. Compared with WT of waves in uncracked beam, if the additional peak is found from WT of measurement signal, it means that there exists the crack in the beam. So the position of the crack can be determined according to the arrival time of the first two waves and additional wave. There are two cases. Case 1, additional peak occurs after the first peak and before the second peak, it means that the crack is between the clamped end and the observation point, so the distance from the observation point is $c_g \Delta t/2$, where Δt is the time interval between the first peak and the additional peak. Case 2, additional peak occurs after the second peak, it means that the crack is between the free end and the observation point, so the distance from the observation point is $c_g \Delta t/2$, where $\Delta t$is the time interval between the second peak and the additional peak.

7. Experimental investigation

The experimental investigation is performed by a cantilever beam with an edge crack subjected to impact at free end. The Plexiglass cantilever beam of 4.09 mm × 32.41 mm cross-section, 260 mm in total length, modulus of elasticity $E = 5.03 \times 10^9$ Pa, the Poisson ratio $\nu = 0.361$, density $\rho = 1215\,\mathrm{kg/m^3}$ and shear force factor $\kappa = \frac{2}{3}$ is only taken in this experiment. The pre-crack with depth 12 mm is located at 107.21 mm from the free end. The bending strains are measured by using strain gages at points C and D with the distance 60 and 180 mm from the free end. The sampling period T is equal to 0.25 μs.

Fig. 8 shows strains measured at positions C and D. Fig. 9 shows the magnitude of WT of strains at positions C and D at normalized scale $a = 200$ (normalized cut-off scale $a_c = 186$). The first peaks of C and D can be detected at 257.5 and 372.25 μs, respectively. According to Eq. (27), group velocity $c_g = 1046\,\mathrm{m/s}$ is given, which agrees well with the theoretical group velocity $c_g = 1081\,\mathrm{m/s}$. Furthermore, the arrival time of the reflected wave at position C from the clamped end is about 639 μs. There is one peak at 639 μs in Fig. 9 for C, which represents reflected wave from the fixed end. Between them, there occur additional peaks (337.5 μs), which include the influence of crack. According to the first peak (257.5 μs) and the additional peak (337.5 μs), the

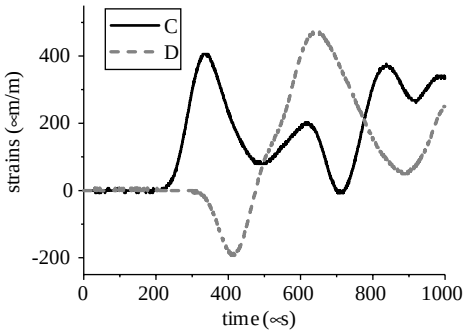

Fig. 8. Strains measured at positions C and D.

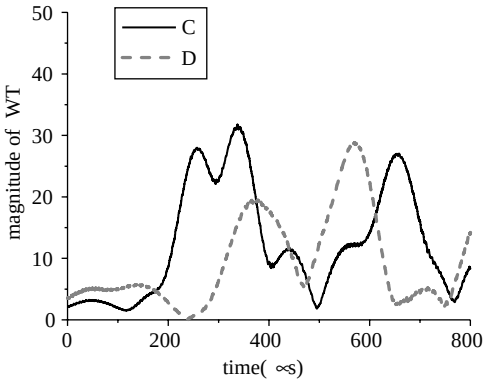

Fig. 9. Magnitude of WT of waves measured at positions C and D.

distance of the crack from position C can be determined at about 43.2 mm (the actual distance is 47.2 mm). According to the WT of position D, the distance of the crack from position C is 43.4 mm. As for the high-frequency wave, it is too weak to distinguish from the noise by wavelet transform. When the scale is too large, that is to say, the frequency is too low, the peaks indicating the wave caused by the crack do not be seen similar with the analytical result because of the effect of diffraction.

Compared with the real condition, it is illustrated that it is an effective method for determining the location of the crack by utilizing mid-frequency flexural wave extracted by wavelet transform.

8. Conclusion

From the analytical and experimental analysis, it is concluded that the model of cracked beam is suitable for the mid-frequency flexural wave. As for the high-frequency flexural wave, the analytical analysis can give good results, but in fact, the signal is too weak to distinguish from the noise. The low-frequency flexural wave also cannot be used to detect the location of the crack because of the effect of diffraction. To utilize the mid-frequency slow wave extracted by wavelet transform to detect the crack can give better results. This method can only determine the existence and location of the crack, which is not suitable for diagnosing the depth of crack and style of damage. So this method can be used as a supplement of the ultrasonic method, so that much time and money will be saved. Furthermore, this method based on mid-frequency flexural wave extracted by wavelet transform is also suitable for the existence and location of multi-crack in the beam.

Acknowledgements

This work is funded by the National Natural Science Foundation of China (No. 19872006) and State Education Commission of China (No. 98000144). Their support and assistance are gratefully acknowledged.

Appendix

The scatter matrix and source vector of Joint J is expressed by, respectively,

$$\boldsymbol{S}^J = -(\boldsymbol{D}^J)^{-1}\boldsymbol{A}^J, \qquad \hat{\boldsymbol{s}}^J = -(\boldsymbol{D}^J)^{-1}\hat{\boldsymbol{g}}^J.$$

For the joint at the crack

$$\boldsymbol{D}^J = \begin{bmatrix} 1+\alpha_1 & 1+\alpha_2 & 1+\alpha_1 & 1+\alpha_2 \\ -\alpha_1 s_1 & -\alpha_2 s_2 & \alpha_1 s_1 & \alpha_2 s_2 \\ s_1^2 & s_2^2 & s_1^2 & s_2^2 \\ -s_1 & -s_2 & -s_1 - Cs_1^2 & -s_2 - Cs_2^2 \end{bmatrix}, \quad \boldsymbol{A}^J = \begin{bmatrix} 1+\alpha_1 & 1+\alpha_2 & 1+\alpha_1 & 1+\alpha_2 \\ \alpha_1 s_1 & \alpha_2 s_2 & -\alpha_1 s_1 & -\alpha_2 s_2 \\ s_1^2 & s_2^2 & s_1^2 & s_2^2 \\ -s_1 & -s_2 & s_1 - Cs_1^2 & s_2 - Cs_2^2 \end{bmatrix},$$

$$\hat{\boldsymbol{g}}^J = (0,0,0,0)^{\mathrm{T}}.$$

For the joint at the clamped end

$$\boldsymbol{D}^J = \begin{bmatrix} 1+\alpha_1 & 1+\alpha_2 \\ s_1 & s_2 \end{bmatrix}, \qquad \boldsymbol{A}^J = \begin{bmatrix} 1+\alpha_1 & 1+\alpha_2 \\ -s_1 & -s_2 \end{bmatrix}, \qquad \hat{\boldsymbol{g}}^J = (0,0)^{\mathrm{T}}.$$

For the joint at the free end

$$\boldsymbol{D}^J = \begin{bmatrix} s_1^2 & s_2^2 \\ -s_1 & -s_2 \end{bmatrix}, \qquad \boldsymbol{A}^J = \begin{bmatrix} s_1^2 & s_2^2 \\ s_1 & s_2 \end{bmatrix}, \qquad \hat{\boldsymbol{g}}^J = (\hat{M}^J, \hat{F}^J)^{\mathrm{T}}.$$

For the joint at the simply supported end

$$\boldsymbol{D}^J = \begin{bmatrix} 1+\alpha_1 & 1+\alpha_2 \\ s_1^2 & s_2^2 \end{bmatrix}, \qquad \boldsymbol{A}^J = \begin{bmatrix} 1+\alpha_1 & 1+\alpha_2 \\ s_1^2 & s_2^2 \end{bmatrix}, \qquad \hat{\boldsymbol{g}}^J = (0, \hat{M}^J)^{\mathrm{T}}.$$

For the general joints

$$\boldsymbol{D}^J = \begin{bmatrix} s_1^2 & s_2^2 & s_1^2 & s_2^2 \\ -\alpha_1 s_1 & -\alpha_2 s_2 & \alpha_1 s_1 & \alpha_2 s_2 \\ 1+\alpha_1 & 1+\alpha_2 & 1+\alpha_1 & 1+\alpha_2 \\ -s_1 & -s_2 & s_1 & s_2 \end{bmatrix}, \qquad \boldsymbol{A}^J = \begin{bmatrix} s_1^2 & s_2^2 & s_1^2 & s_2^2 \\ \alpha_1 s_1 & \alpha_2 s_2 & -\alpha_1 s_1 & -\alpha_2 s_2 \\ 1+\alpha_1 & 1+\alpha_2 & 1+\alpha_1 & 1+\alpha_2 \\ s_1 & s_2 & -s_1 & -s_2 \end{bmatrix},$$

$$\hat{\boldsymbol{g}} = (\hat{M}^J, \hat{F}^J, 0, 0)^{\mathrm{T}},$$

where $\hat{M}^J$and $\hat{F}^J$are the external moment and vertical force of Joint J, respectively.

References

[1] Y. Zou, L. Tong, G.P. Steven, Vibration-based model dependent damage (delamination) identification and health monitoring for composite structures: a review, Journal of Sound and Vibration 230 (2) (2000) 357–378.

[2] W.M. Ostachouitz, M. Krawczuk, Analysis of the effect of cracks on the natural frequencies of a cantilever beam, Journal of Sound and Vibration 150 (2) (1991) 191–201.

[3] P.F. Rizos, N. Aspragathos, Identification of crack location and magnitude in a cantilever beam from the vibration modes, Journal of Sound and Vibration 138 (3) (1990) 381–388.

[4] Y. Narkis, Identification of crack location in vibration simply supported beams, Journal of Sound and Vibration 172 (4) (1994) 549–558.

[5] E.I. Shifrin, R. Routolo, Natural frequencies of a beam with an arbitrary number of crack, Journal of Sound and Vibration 222 (3) (1999) 409–423.

[6] M. Hongwei, Y. Guitong, The method and progress of the non-destructive test of the structure. Progress in Mechanics (in Chinese), Progress in Mechanics 29(4) (1999) 513–527.

[7] H. Inoue, K. Kishimoto, T. Shibuya, Experimental wavelet analysis of flexural waves in beams, Experimental Mechanics 36 (3) (1996) 212–217.

[8] T. Onsay, A. Haddow, Wavelet transform analysis of transient wave propagation in a dispersive medium, Journal of Acoustical Society of America 95 (3) (1994) 1441–1449.

[9] S.M. Howard, Y.H. Pao, Analysis and experiment on stress waves in planar trusses, Journal of Engineering Mechanics, American Society of Mechanical Engineers 124 (3) (1998) 884–891.

[10] J. Tian, X. Su, Transient axisymmetric elastic waves in finite orthotropic cylindrical shells, Universitatis Pekinensis (Acta Scientiarum Naturalium) 36 (3) (2000) 365–372.